JOURNAL OF GEOPHYSICAL RESEARCH, VOL. 106, NO. B8, PAGES 16,499-16,513, AUGUST 10, 2001

# Hillslope evolution by nonlinear, slope-dependent transport: Steady state morphology and equilibrium adjustment timescales

Joshua J. Roering,[1] James W. Kirchner, and William E. Dietrich

Department of Earth and Planetary Science, University of California, Berkeley, California

**Abstract.** Soil-mantled hillslopes are typically convex near the crest and become increasingly planar downslope, consistent with nonlinear, slope-dependent sediment transport models. In contrast to the widely used linear transport model (in which sediment flux is proportional to slope angle), nonlinear models imply that sediment flux should increase rapidly as hillslope gradient approaches a critical value. Here we explore how nonlinear transport influences hillslope evolution and introduce a dimensionless parameter $\Psi_L$ to express the relative importance of nonlinear transport. For steady state hillslopes, with increasing $\Psi_L$ (i.e., as slope angles approach the threshold angle and the relative magnitude of nonlinear transport increases), the zone of hillslope convexity becomes focused at the hilltop and side slopes become increasingly planar. On steep slopes, rapid increases in sediment flux near the critical gradient limit further steepening, such that hillslope relief and slope angle are not sensitive indicators of erosion rate. Using a one-dimensional finite difference model, we quantify hillslope response to changes in baselevel lowering and/or climate-related transport efficiency and use an exponential decay function to describe how rapidly sediment flux and erosion rate approach equilibrium. The exponential timescale for hillslope adjustment decreases rapidly with increasing $\Psi_L$. Our results demonstrate that the adjustment timescale for hillslopes characteristic of the Oregon Coast Range and similar steep, soil-mantled landscapes is relatively rapid ($\leq$ 50 kyr), less than one quarter of the timescale predicted by the linear transport model.

## 1. Introduction

The morphology of landscapes reflects the integrated effect of tectonic and climatic forcing as regulated by surface processes. Although numerous studies have used topographic data to explore landscape dynamics and infer rates of uplift and erosion from morphologic properties of drainage basins [e.g., *Ahnert*, 1970; *Milliman and Syvitski*, 1992; *Granger et al.*, 1996; *Hurtrez et al.*, 1999], the variability of surface processes, climate, and uplift rates often confounds such investigations [*Riebe et al.*, 2000]. In order to systematically analyze how crustal deformation and climate change may affect landscape properties, such as relief, drainage density, and the distribution of regolith, the relevant sediment transport processes must be well characterized.

In mountainous landscapes, landsliding and mass wasting dominate sediment transport on hillslopes [e.g., *Strahler*, 1950; *Carson and Petley*, 1970; *Burbank et al.*, 1996]. The frequency and magnitude of these slope-dependent processes control hillslope morphology as well as the time required for hillslopes to adjust to changes in the rate of channel incision or climate-related transport efficiency. Owing to the difficulty in obtaining field-calibrated hillslope erosion models many fundamental relationships between hillslope processes and landscape dynamics have been unexplored. For example, how does the response to an increase in baselevel lowering differ for steep, landslide-prone slopes and gentle, soil creep-dominated hillslopes? Also, does the relief associated with individual hillslopes control mountain-scale relief?

Soil-mantled hillslopes (on which erosion rates do not exceed the rate at which bedrock is converted to soil [e.g., *Heimsath et al.*, 1997]) are found in hilly and mountainous landscapes throughout the world and tend to have a characteristic convex form, suggesting erosion by a common mechanism. *Davis* [1892] and *Gilbert* [1909] recognized the paucity of overland flow erosion on convex hillslopes and suggested that downslope soil creep is controlled by disturbance-driven processes (e.g., biogenic activity and wet/dry cycles) such that sediment transport rates should depend primarily on gravity and thus hillslope gradient. Since the seminal work of *Gilbert* [1909], the linear, slope-dependent transport model has often been used to simulate hillslope erosion [e.g., *Culling*, 1960; *Kirkby*, 1971; *Koons*, 1989; *Tucker and Slingerland*, 1994], but the morphology of most soil-mantled hillslopes is inconsistent with the constant-curvature form predicted by the linear model under steady state erosion. Instead, soil-mantled hillslopes tend to be convex near the crest (or drainage divide) and become increasingly planar downslope [*Anderson*, 1994; *Howard*,

[1]Now at Department of Geological Sciences, University of Oregon, Eugene, Oregon



Paper number 2001JB000323.
0148-0227/01/2001JB000323$09.00

1994; *Roering et al.*, 1999]. This observation, coupled with results from topography-based erosion modeling in the Oregon Coast Range, indicates that nonlinear sediment transport models may be more appropriate than the linear model for simulating the erosion of soil-mantled hillslopes [*Roering et al.*, 1999]. According to nonlinear models, which are also supported by recent experimental results [*Roering et al.*, 2001], sediment flux is linearly related to hillslope gradient at low angles and increases rapidly as slope angles approach a critical value related to the angle of repose [*Kirkby*, 1984; *Anderson*, 1994; *Howard*, 1994; *Roering et al.*, 1999]. This behavior has important yet unexplored implications for how hillslopes respond to changes in uplift rate and/or climatic variables.

Ever since *Hack* [1960] elaborated *Gilbert*'s [1877] hypothesis that landscapes tend to adjust their form such that erosion rates are spatially constant, numerous studies have used the equilibrium conceptual framework to guide their investigations of landscape evolution [e.g., *Brunsden and Lin*, 1991; *Reneau and Dietrich*, 1991; *Burbank et al.*, 1996; *Hovius et al.*, 1997; *Meigs et al.*, 1999; *Whipple et al.*, 1999; *Riebe et al.*, 2000]. Field evidence demonstrating an approximate balance between uplift and erosion is difficult to obtain owing to variability in temporal and spatial scales of observation. As a result, theoretical models have often been used to simulate how tectonic forcing and other factors may influence landscape evolution [e.g., *Ahnert*, 1976; *Koons*, 1989; *Willgoose et al.*, 1991; *Rinaldo et al.*, 1995; *Fernandes and Dietrich*, 1997; *Howard*, 1997]. The time required for hillslopes to adjust to tectonic and climatic forcing affects the dynamics of mountain-scale erosion, the potential for isostatic unloading, the rate and characteristics of sediment supply to channels, and the development of relief. Recent advances in formulating mechanistic, calibrateable sediment transport models have enabled geomorphologists to quantitatively explore how landscapes may respond to changing boundary conditions. Using numerical simulations, *Fernandes and Dietrich* [1997] systematically analyzed how the linear transport model influences transient hillslope response. Following stepwise changes in baselevel lowering rate and/or climate-related transport efficiency, *Fernandes and Dietrich* [1997] quantified the time necessary for erosion and sediment transport rates to adjust within an arbitrary percentage of the new equilibrium value. This contribution expands upon *Fernandes and Dietrich*'s [1997] study by (1) using an exponential decay function to provide a more detailed and useful description of hillslope adjustment to changing boundary conditions and (2) investigating how nonlinear sediment transport influences hillslope adjustment and evolution. In addition, we use analytical solutions for equilibrium hillslope morphology to explore how baselevel lowering rates affect steady state hillslope morphology and relief in our Oregon Coast Range study site. We demonstrate that the adjustment timescale decreases rapidly as the importance of nonlinear sediment transport increases.

## 2. Modeling Slope-Dependent Sediment Transport on Hillslopes

Ever since *Davis* [1892] and *Gilbert*'s [1909] rationalization for the convex form of hilltops, sediment transport on soil-mantled hillslopes has been modeled as a slope-dependent process [e.g., *Kirkby*, 1971; *Ahnert*, 1976; *Howard*, 1994; *Dietrich et al.*, 1995]. Through analogy with *Fourier*'s [1822] heat conduction equation (in which heat flux is proportional to thermal gradient), *Culling* [1960] modeled hillslope evolution using the linear sediment transport model, such that sediment flux $\tilde{q}$ is proportional to hillslope gradient:

$$\tilde{q} = -K\nabla z \tag{1}$$

where $K$ is a rate constant ($L^2\ T^{-1}$) and $z$ is elevation above an arbitrary datum ($L$). Sediment transport rates on low-gradient hillslopes have been estimated from analyses of cosmogenic radionuclides and are consistent with (1) [*McKean et al.*, 1993; *Small et al.*, 1999]. However, a recent topographic study indicates that nonlinear sediment transport models [*Anderson*, 1994; *Howard*, 1994] may be more appropriate for simulating the erosion of entire hillslopes [*Roering et al.*, 1999]. Generally, these nonlinear models include a critical gradient term that generates high sediment fluxes on steep slopes and thus limits further hillslope steepening. According to a proposed nonlinear model [*Andrews and Bucknam*, 1987; *Roering et al.*, 1999], sediment flux varies with gradient according to

$$\tilde{q} = \frac{-K\nabla z}{1-\left(|\nabla z|/S_c\right)^2} \tag{2}$$

where $S_c$ is the critical gradient. Equation (2) is similar to (1) when $|\nabla z| << S_c$, but as $|\nabla z|$ approaches $S_c$, sediment flux increases rapidly, becoming infinite when $|\nabla z| = S_c$ (Figure 1). This model does not explicitly account for landslides, but as $|\nabla z|$ approaches $S_c$, (2) may effectively capture the behavior of

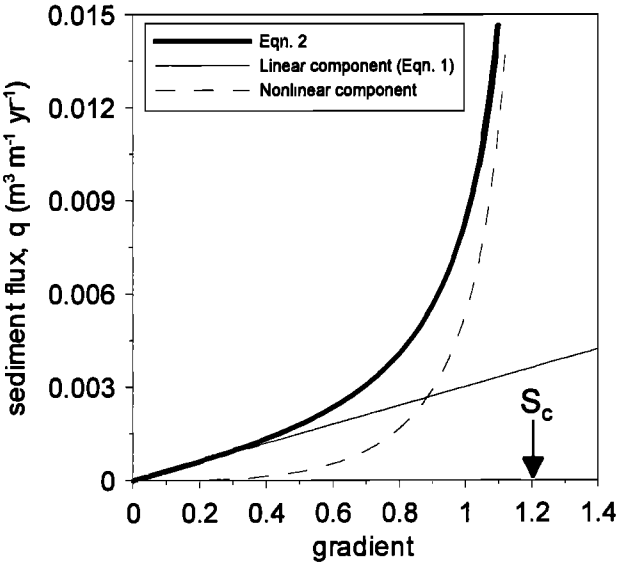


**Figure 1.** Theoretical relationship between hillslope gradient and sediment flux. The thick line indicates total sediment flux calculated with (2) ($K$=0.003 m$^2$ yr$^{-1}$ and $S_c$=1.2), which can be divided into linear (thin line) and nonlinear (dashed line) components (equation (7)). We distinguish the linear and nonlinear components to quantify the relative importance of nonlinear transport on hillslopes (equation (8)), but do not suggest that these two components represent distinct processes (see text).

small landslides that are not triggered by the topographic convergence of subsurface flow and do not travel long distances through the channel network [*Roering et al.*, 1999].

Sediment flux and landscape lowering can be related through the continuity equation:

$$\rho_s \frac{\partial z}{\partial t} = -\rho_s \nabla \cdot \tilde{q} + \rho_r C_o(t) \tag{3}$$

where $C_o(t)$ is the time-dependent rate of rock uplift, which we define as equivalent to the baselevel lowering (or channel incision) rate along the hillslope margin ($L\ T^{-1}$), and $\rho_r$ and $\rho_s$ are the bulk densities of rock and sediment ($M\ L^{-3}$), respectively. If $C_o(t)$ is finite and does not vary with time, hillslopes may approach an approximate steady state, such that across the hillslope, $\partial z/\partial t \cong 0$ and $\rho_r C_o \cong \rho_s \nabla \cdot \tilde{q}$. In this paper, we will explore steady-state hillslope morphology and hillslope response to changes in baselevel lowering, $C_o(t)$, and climate change (which we model by changing the transport rate constant $K$).

To focus our investigation of how nonlinear transport affects hillslope morphology and equilibrium adjustment timescales, we use a simple, one-dimensional (i.e., profile) analysis. Although two-dimensional analyses of (1) and (2) are computationally feasible, they require that we specify models governing channel formation (e.g., fluvial erosion or debris flow incision [*Howard and Kerby*, 1983; *Whipple and Tucker*, 1999]), which control channel network geometry and thus the spatial scale of hillslopes. In addition, the inclusion of channel-forming processes requires additional model formulation and parameterization which unnecessarily complicate our analysis. *Howard* [1997] compared landscape evolution simulations using hillslope and fluvial transport models and demonstrated that one-dimensional simulations capture similar characteristics as their two-dimensional counterparts. His results indicated that the influence of erosion rate on drainage density (and thus average hillslope length) depends strongly on the chosen model for fluvial erosion [*Howard*, 1997]. By not including valley-forming processes and their complex dependencies, our simple hillslope profile analysis allows us to focus on hillslope response to changes in the rate of baselevel lowering and/or climate-induced changes in transport efficiency.

The length scale of our one-dimensional model hillslopes should scale with the drainage area per unit contour width, $a/b$ ($L$), which defines the hillslope-valley transition as defined in two-dimensional hillslope representations [e.g., *Tucker and Bras*, 1998; *Roering et al.*, 1999]. Analyses of channel initiation indicate that a threshold defined by gradient and $a/b$ may control the transition from hillslopes to the valley network [e.g., *Dietrich et al.*, 1992; *Montgomery and Dietrich*, 1992]. Thus our investigation only applies to hillslopes whose length scale $L_h$ is less than the average value of $a/b$ required to form channels or valleys. The channelization threshold may also vary with lithologic and climatic variables [*Montgomery and Dietrich*, 1989].

## 3. Steady State Hillslope Morphology

### 3.1. Nonlinear and Linear Transport Models

Using the equilibrium assumption ($\partial z/\partial t \cong 0$) and (3), we can quantify the equilibrium morphology of hillslopes that erode according to linear and nonlinear transport models. By substituting (1) and (2) into the one-dimensional version of (3), respectively, we obtain expressions relating profile curvature to the baselevel lowering rate for the linear and nonlinear models, respectively:

$$\frac{d^2z}{dx^2} = \frac{-\beta}{K} \tag{4a}$$

$$\frac{d^2z}{dx^2} = \frac{-\beta}{K}\left(1-\left(\frac{dz/dx}{S_c}\right)^2\right)^2 \Bigg/ \left(1+\left(\frac{dz/dx}{S_c}\right)^2\right) \tag{4b}$$

where $\beta=(\rho_r/\rho_s)C_o$ and $x$ is horizontal distance from the drainage divide or hillslope crest. Whereas linear transport (equation (4a)) predicts that hillslope curvature should be constant across hillslopes, nonlinear transport (equation (4b)) implies that hillslope convexity should be greatest when $dz/dx$ equals zero and decreases continuously with slope, approaching zero as $dz/dx$ approaches $S_c$. By integrating (4a) and (4b) with respect to $x$ we can quantify the spatial variation of hillslope gradient for the linear and nonlinear models, respectively:

$$\frac{dz}{dx} = \frac{-\beta}{K}x + c_1 \tag{5a}$$

$$\frac{dz}{dx} = \frac{S_c^2}{2\beta x}\left[-K + \sqrt{K^2 + \left(\frac{2\beta x}{S_c}\right)^2}\right] + c_2 \tag{5b}$$

where $c_1$ and $c_2$ are constants of integration. For both (5a) and (5b) we define $x=0$ as the hillslope crest, such that $dz/dx$ approaches zero with diminishing $x$ and $c_1=c_2=0$. The linear model (equation (5a)) predicts that equilibrium hillslope gradients increase linearly downslope, whereas on sufficiently long hillslopes ($x >> KS_c/2\beta$) the nonlinear model (equation (5b)) predicts that hillslope gradients increase nonlinearly, approaching $S_c$ downslope of the drainage divide. By integrating these equations once more, we can derive expressions for equilibrium elevation profiles, under the linear and nonlinear models, respectively:

$$z = \frac{-\beta}{2K}x^2 + c_3 \tag{6a}$$

$$z = \frac{-S_c^2}{2\beta}\left[\sqrt{K^2 + (2\beta x/S_c)^2} - K\ln\left(\frac{\sqrt{K^2 + (2\beta x/S_c)^2} + K}{2\beta/S_c}\right)\right] + c_4 \tag{6b}$$

We do not include expressions for the constants of integration, $c_3$ and $c_4$, because they arbitrarily define the absolute value of elevation at the hillslope crest, whereas our analysis only seeks to characterize the relative variation of elevation across model hillslopes.

### 3.2. Quantifying the Relative Importance of Nonlinear Transport

Numerous studies have explored the characteristics of equilibrium hillslope morphology as modeled by the linear transport model ((4a), (5a), and (6a)) [*Kirkby*, 1971; *Koons*,

1989; *Fernandes and Dietrich*, 1997]. *Dietrich and Montgomery* [1998] demonstrated that landslide-driven transport may influence relief, but we are unaware of studies that have systematically analyzed how nonlinear transport affects hillslope relief, gradient, and curvature. Our nonlinear transport model (equation (2)) can be rewritten as the combination of two flux terms, a purely linear component $q_{lin}$ and a nonlinear component $q_{non}$ (Figure 1):

$$q = q_{lin} + q_{non} = K\frac{dz}{dx} + \frac{K\dfrac{dz}{dx}\left(\dfrac{dz/dx}{S_c}\right)^2}{1-\left(\dfrac{dz/dx}{S_c}\right)^2} \tag{7}$$

By this conceptual framework we are not implying that two distinct transport mechanisms combine to generate the nonlinear sediment flux relationship quantified by (2). On the contrary, the formulation of (2) assumes only that the work done on hillslopes by disturbance-driven processes is balanced by frictional and gravitational forces and no additional processes are invoked to generate the nonlinearity [*Roering et al.*, 1999]. In order to guide our theoretical analysis, we introduce a dimensionless ratio $\Psi$ that quantifies the relative importance of nonlinear sediment flux at an arbitrary point along a hillslope. We define $\Psi$ as the ratio of nonlinear to linear components of sediment flux calculated at an arbitrary location along the hillslope ($x$) according to

$$\Psi = \left.\frac{q_{non}}{q_{lin}}\right|_x = \left.\frac{\left(\dfrac{dz/dx}{S_c}\right)^2}{1-\left(\dfrac{dz/dx}{S_c}\right)^2}\right|_x \tag{8a}$$

For an equilibrium hillslope, $\Psi$ increases downslope as slope gradients increase and the nonlinear component of sediment flux increases more rapidly than the linear component. For all of our analyses we evaluate $\Psi$ at the base (or channel margin) of our modeled hillslopes ($\Psi_L=\Psi(L_h)$, where $L_h$ is hillslope length), by substituting (5b) into (8a):

$$\Psi_L = \frac{\left\{\dfrac{S_c}{2\beta L_h}\left[-K+\sqrt{K^2+\left(\dfrac{2\beta L_h}{S_c}\right)^2}\right]\right\}^2}{1-\left\{\dfrac{S_c}{2\beta L_h}\left[-K+\sqrt{K^2+\left(\dfrac{2\beta L_h}{S_c}\right)^2}\right]\right\}^2} \tag{8b}$$

The nonlinear transport ratio $\Psi_L$ quantifies the relative importance of nonlinear transport at the hillslope base. As a result, $\Psi_L$ is a measure of the magnitude and distribution of hillslope convexity.

## 4. Study Site: Oregon Coast Range

Our investigation of hillslope morphology and evolution is motivated by data and observations from the central Oregon Coast Range (OCR), although our analysis may be applied to most soil-mantled hillslopes. The OCR is a humid, forested, mountainous landscape whose central and southern regions are underlain by a thick section of Eocene turbidites mapped as the Tyee Formation [*Baldwin*, 1956; *Snavely et al.*, 1964; *Heller et al.*, 1985]. The Tyee Formation has been compressed into a series of low-amplitude, north-northeast striking folds that seldom exhibit dip angles greater than 20° [*Baldwin*, 1956]. The Oregon Coast Range is situated above a subduction zone and has experienced uplift over the last 20-30 Myr [*Orr et al.*, 1992].

Much of the terrain in the Oregon Coast Range is characterized by steep, highly dissected, soil-mantled mountains and incised bedrock river valleys (Figure 2).

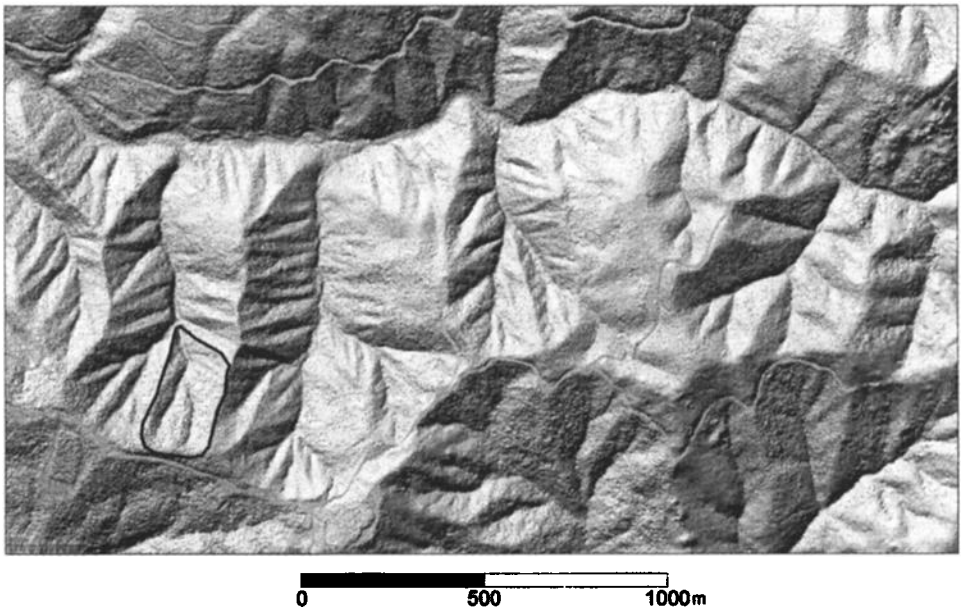


**Figure 2.** Shaded relief map of study site near Coos Bay, Oregon. Topographic data were obtained with airborne laser altimetry at an average spacing of 2.3 m. The dark line delineates a small basin used in Figure 3. Modified from *Roering et al.* [1999].

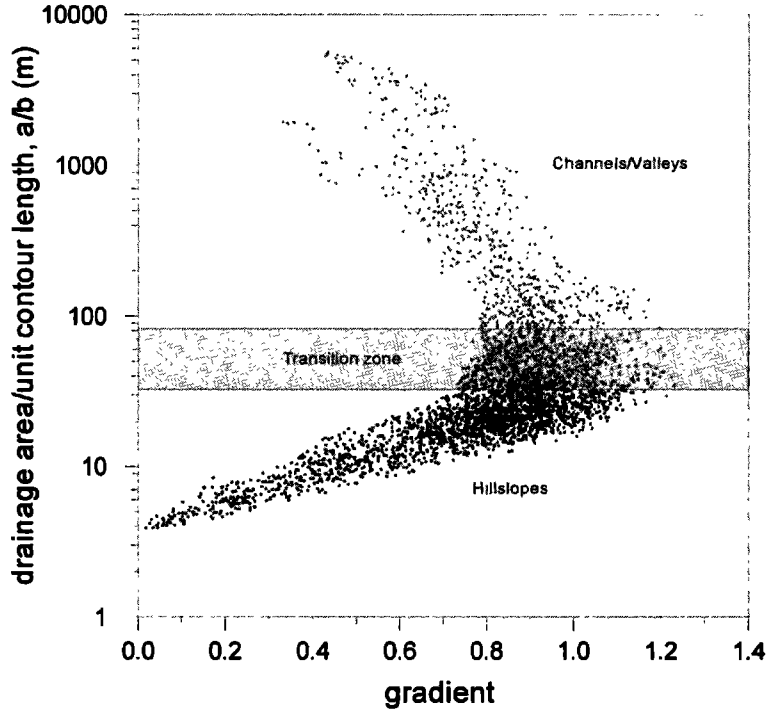


**Figure 3.** Semilog plot showing the relationship between drainage area per unit contour ($a/b$) and gradient for the basin delineated in Figure 2. The gray band signifies the transition zone between hillslopes and the valley network and thus defines the average length scale of hillslopes in our study area. Solid and shaded circles denote divergent (curvature < 0) and convergent (curvature > 0) portions of the landscape, respectively. Modified from *Roering et al.* [1999].

Alternating ridges and unchanneled valleys dominate the topography and have a relatively uniform spacing [*Dietrich and Dunne*, 1978; *Montgomery and Dietrich*, 1989; *Benda and Dunne*, 1997]. Thin soils typically mantle ridges, and thick colluvial deposits fill unchanneled valleys at the uppermost extent of the channel network. Our proposed transport model (equation (2)) applies to purely slope-dependent transport processes on divergent and planar hillslopes but does not encompass debris flow processes or deep-seated landsliding. Denudation rates (~ 0.07-0.1 mm yr $^{-1}$) do not vary significantly with spatial scale, such that an approximate equilibrium may exist between sediment production on hillslopes and basin-wide sediment yield [*Reneau and Dietrich*, 1991; *Heimsath*, 1999]. In our study area, high-resolution topographic data were obtained using airborne laser altimetry, which can accurately characterize fine-scale topographic features over large areas (see Figure 2).

In this study, we used parameters characteristic of the OCR study site, where *Roering et al.* [1999] calibrated $K$ and $S_c$ using topographic data ($K$=0.003 m$^2$ yr$^{-1}$ and $S_c$=1.2). To characterize the transition from hillslopes to the valley-channel network and estimate the average hillslope length, we used high-resolution topographic data from a small catchment in our study site near Coos Bay, Oregon (see Figure 2), to plot topographic gradient versus drainage area per unit contour length ($a/b$). Hillslopes are characterized by small $a/b$ and generally exhibit a trend of increasing $a/b$ with gradient (Figure 3). For $a/b$ greater than ~ 80 m, $a/b$ decreases with gradient, thereby distinguishing the valley network. As a result, $a/b \cong$30-80 m defines the transition between hillslopes and the valley network and thus denotes the average spatial scale of hillslopes (see shaded band on Figure 3). Much of the variability in this transition zone results from the influence of valley gradient on valley formation, such that valley heads with smaller drainage areas are typically steeper than those with larger drainage areas [*Montgomery and Dietrich*, 1992]. In our study site, most of the hillslopes terminate into steep valleys (or hollows), so we chose $L_h$=40 m as the average hillslope length for our simulations.

## 5. Characteristics of Equilibrium Hillslope Morphology

### 5.1. Nonlinear Transport and Hillslope Convexity

Using (4b), (5b), and (6b), we can analyze how nonlinear sediment transport influences steady state hillslope morphology. Figure 4 illustrates how varying $\Psi_L$ affects hillslope elevation, gradient, and curvature profiles calculated for a theoretical hillslope with arbitrary length and erosion rate ($L_h$=40 m; $C_o$=0.5x10$^{-4}$ m yr$^{-1}$; $\rho_r/\rho_s$=2.0). To clarify how $\Psi_L$ affects hillslope morphology, we used (5b) and (8b) conjointly, systematically varying $K$ and $S_c$ to generate hillslope gradient profiles with varying $\Psi_L$ and a constant gradient of 1.0 at the hillslope base (Figure 4b). For each value of $\Psi_L$ we used the corresponding values of $K$ and $S_c$ to calculate elevation and curvature profiles using (4b) and (6b) (Figures 4a and 4c). In effect, $\Psi_L$ quantifies the distribution and magnitude of hillslope convexity. For hillslopes without a critical gradient constraint ($S_c$=$\infty$ and $\Psi_L$=0), gradient increases linearly from the crest and curvature is spatially constant (as predicted by (4a) and (4b)). For $\Psi_L$=1 the

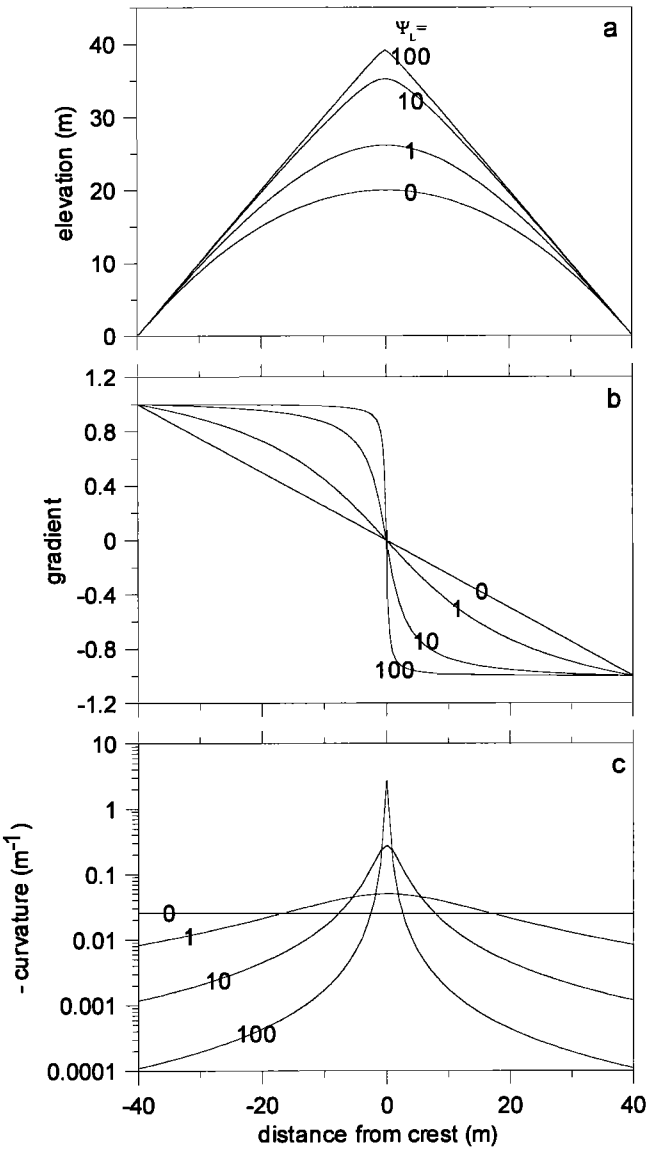


**Figure 4.** Profiles of (a) elevation, (b) gradient, and (c) curvature for equilibrium hillslopes modeled with (4b), (5b), and (6b). Each hillslope has a constant lowering rate $C_o$ equal to $1.0\text{x}10^{-4}$ m yr$^{-1}$, and the labels refer to the value of $\Psi_L$ for that hillslope. To most clearly illustrate how $\Psi_L$ influences morphology, we set the gradient equal to 1.0 at the base of each hillslope and varied the values of $K$ and $S_c$ to generate the modeled profiles. For $\Psi_L$=0, hillslope profiles are parabolic (and thus have constant curvature as expected for the linear model). With increasing $\Psi_L$, the zone of hillslope convexity becomes narrower, and the magnitude of the hilltop convexity increases (see Figure 4c), whereas side slopes become increasingly planar. For very large $\Psi_L$ the hillslope approximates an "angle of repose" hillslope with effectively straight, uniform gradient slopes.

nonlinear and linear components of sediment flux at the base of the hillslope are equal, such that much of the upslope hillslope area is dominated by the linear transport component (Figure 4). As a result, such hillslopes exhibit relatively little variation in curvature (relative to cases where $\Psi_L$>1). With increasing $\Psi_L$, side slopes of modeled hillslopes become increasingly planar, and convexity becomes increasingly concentrated at hilltops. Such "convexoplanar" slopes are characteristic of hillslopes in the Oregon Coast Range study site, for which $\Psi_L$ is approximately equal to 1.8 (equation (8b)). For $\Psi_L$ >>1 the modeled hillslope approximates an "angle of repose" slope with effectively planar side slopes and an extremely narrow convexity (i.e., a sharp peak) at the divide.

### 5.2. Hillslope Gradient, Relief, and Curvature in the Oregon Coast Range

To explore how nonlinear transport influences linkages between landscape morphology and tectonic forcing, we used both the linear and nonlinear transport models ((4)-(6)) to quantify morphologic properties of equilibrium hillslopes for varying erosion rates. Holding other factors equal (e.g., the influence of erosion rate on drainage spacing [*Howard*, 1997]) and using our calibrated OCR parameters ($K$=0.003 m$^2$ yr$^{-1}$, $S_c$=1.2, $L_h$=40m, and $\rho_r/\rho_s$=2.0), Figure 5 illustrates how varying the erosion rate $C_o$ (or rate of tectonic forcing) influences maximum and average hillslope gradient, hilltop curvature, and relief for the linear and nonlinear transport models. Values of hilltop curvature (calculated at $x$=0, such that $dz/dx$=0) were calculated using (4a) and (4b), and the maximum and average gradients were calculated using (5a) and (5b). Hillslope relief $H$ is calculated from (6a) and (6b), as $H=z(0)-z(L_h)$. For very low erosion rates ($C_o < 5\text{x}10^{-5}$ m yr$^{-1}$ and $\Psi_L$<1 ) the linear and nonlinear models give similar results, predicting that the average and maximum hillslope gradients and hillslope relief increase linearly with erosion rate. With the linear model, slope angle and relief increase proportionally with erosion rate, suggesting that erosion rates or tectonic forcing can be inferred from hillslope morphology [*Koons*, 1989]. The linear model predicts that relatively long hillslopes exhibit extremely steep slope angles (>60°-70°) near the channel margin, inconsistent with field observations in soil-mantled landscapes.

Contrary to the linear model, (5b) and (6b) imply that hillslope relief and gradient will not be sensitive indicators of uplift (or landscape erosion) rate. For erosion rates higher than $1.0\text{x}10^{-4}$ m yr$^{-1}$ (or $\Psi_L$>1), gradients calculated with the nonlinear model become relatively constant with erosion rate, making slope angle an insensitive indicator of uplift or erosion rate. Similarly, the nonlinear model predicts that hillslope relief becomes relatively independent of erosion rate for $C_o$>$1.0\text{x}10^{-4}$ m yr$^{-1}$ (Figure 5b). For erosion rates characteristic of the Oregon Coast Range, our results indicate that hillslope relief will increase only 10% for a twofold increase in erosion rate. The difference between hillslope relief predicted by the linear and nonlinear transport models increases rapidly with erosion rate, and for our OCR parameters, hillslope relief calculated with the linear model is more than a factor of 2 greater than the nonlinear-derived relief (see Figure 5b).

Despite the discrepancies between nonlinear and linear transport models, both predict that hilltop curvature (calculated where $dz/dx$=0) varies proportionally with erosion rate ((4a) and (4b); see Figure 5a), making it a potentially useful diagnostic tool for inferring tectonic forcing from landscape morphology [e.g., *Roering et al.*, 1999]. Most topographic data, however, are not sufficient to resolve hilltop curvature. In many soil-mantled landscapes, meter-scale

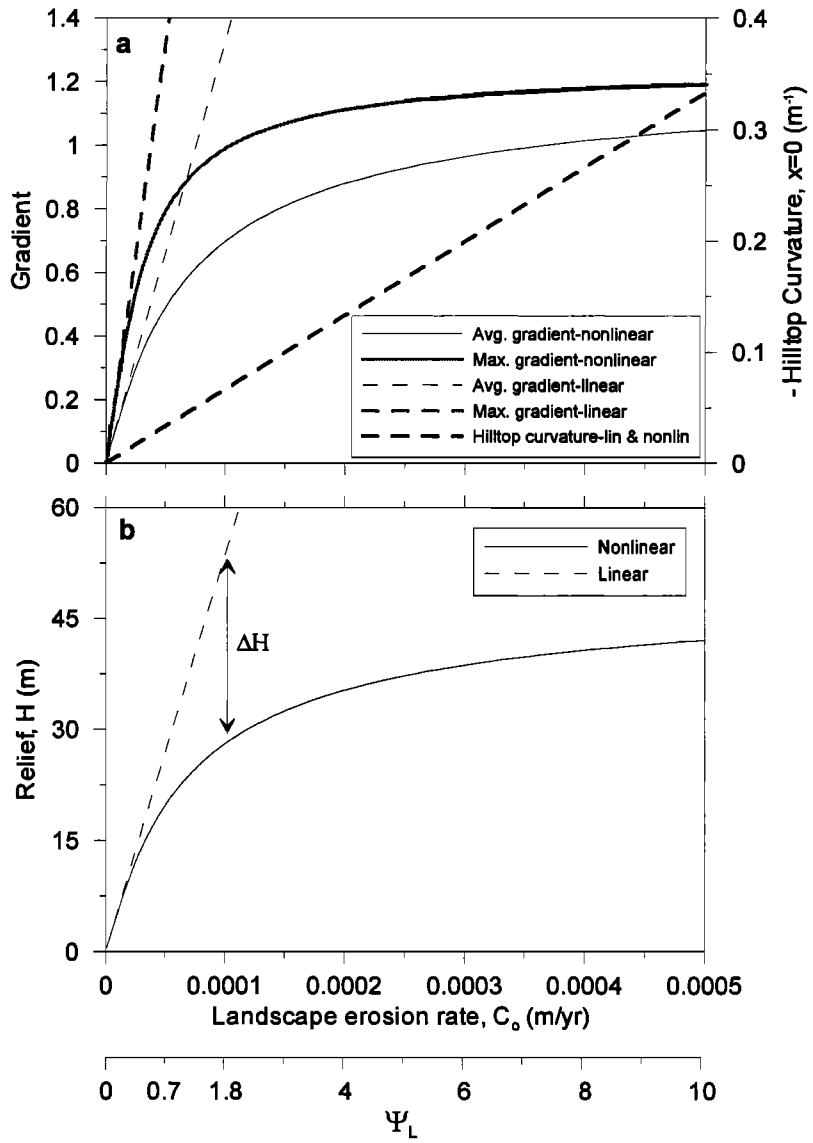


**Figure 5.** Theoretical relationships between morphologic properties and lowering rate for equilibrium hillslopes that erode according to linear and nonlinear transport models ((1) and (2)). (a) Average and maximum gradients increase linearly with lowering rate for linear transport (dashed lines), whereas for nonlinear transport both average and maximum gradient (thin solid and thick shaded lines) become relatively independent of erosion rate and approach $S_c$ as $C_o$ approaches $\infty$. These relationships are calculated with parameters characteristic of our study site in the Oregon Coast Range (OCR) ($K$=0.003 m$^2$ yr$^{-1}$, $S_c$=1.2, $\rho_r/\rho_s$=2.0, and $L_h$=40m). Both linear and nonlinear transport indicate that hilltop curvature (thick solid line) varies proportionally with lowering rate. (b) Relief for the same parameters used above, which increases proportionally with erosion rate for linear transport (dashed lines) and is relatively independent of erosion rate for nonlinear transport (solid lines). The $\Psi_L$ axis illustrates how erosion rate increases the relative magnitude of nonlinear transport on hillslopes (equation (8b)). For small $\Psi_L$, transport is essentially linear, but as $\Psi_L$ gets large, nonlinear transport becomes important, and the disparity between morphology predicted by the linear and nonlinear models increases. $\Delta H$ indicates the difference between hillslope relief predicted with the linear and nonlinear models for the OCR study site.

topographic data (<5 m spacing) are required to characterize hilltop curvature at the appropriate scale.

Nonlinear sediment transport has important implications for the development of hillslope relief, but it is unknown how the relief associated with individual hillslopes compares to the total landscape relief of our Oregon Coast Range study area. Using high-resolution topographic data for our study site, we estimated the scale-dependence of topographic relief to quantify the contribution of individual hillslopes to the total relief. Specifically, we calculated the maximum elevation difference (relief) within a window of fixed radius at evenly spaced intervals across the landscape, thereby generating a distribution of relief for a given spatial scale (window radius). By repeating this process with varying window radii, we characterized the influence of spatial scale on topographic relief. Figure 6 shows that the topographic relief associated with hillslopes in our study site (radius ranging from 20 to 50 m) is ~ 30-60 m, consistent with predictions from our profile

calculation for $C_o \cong 1 \times 10^{-4}$ m yr$^{-1}$ (see Figure 5b). On average, individual hillslope relief accounts for ~ 15-20% of the large-scale relief (~250-300 m) of our study area (Figure 6).

## 6. Timescales of Hillslope Adjustment to Tectonic and Climatic Forcing

### 6.1. Model Description

Hillslopes respond to changes in tectonic and/or climatic forcing by adjusting their morphology and sediment production. The time required for a hillslope to adjust its morphology to a change in baselevel lowering or climate has been termed the "relaxation" or "adjustment" timescale [e.g., *Ahnert*, 1987; *Howard*, 1988]. Numerous theoretical contributions demonstrate that regardless of their initial conditions, model hillslopes evolve asymptotically toward a steady state, such that hillslope characteristics are effectively time-invariant if downcutting rates and model parameters are constant over timescales that are long compared to the hillslope adjustment time [e.g., *Ahnert*, 1987; *Fernandes and Dietrich*, 1997; *Howard*, 1997]. In the following analyses, we consider hillslope adjustment to changes in (1) baselevel lowering $C_o$ and (2) climate-related transport efficiency on hillslopes (which may be realized through the hillslope transport rate constant $K$). The tectonic evolution of mountainous terrain may affect rates of baselevel lowering, and climate change may affect channel incision rates as well as biological communities, including trees and mammals that control disturbance-driven soil transport on hillslopes.

To quantify time-dependent hillslope evolution, we combined (2) and (3) and calculated the spatial and temporal variation of hillslope elevation in one dimension using a finite difference model. For all simulations, we used a small node spacing relative to the total hillslope length. In addition, we implemented an adaptive time step algorithm to maximize efficiency and ensure numerical stability [*Press et al.*, 1992]. For all simulations, we modeled a symmetric hillslope with a crest in the middle and channel margins on either end, where boundary conditions of baselevel lowering (or channel incision) $C_o(t)$ were imposed. Our simulations assumed transport-limited conditions, such that erosion rates do not exceed rates of soil production; the influence of soil production will be explored in future contributions. Although initial conditions have important influences on landscape evolution, they are typically difficult to characterize. Instead of making arbitrary assertions about initial conditions, we used an equilibrium hillslope (calculated using (6b)) as the initial condition for all of our simulations. Specifically, we analyzed how a steady state hillslope evolves toward a new steady state due to an imposed step change in $C_o$ or $K$.

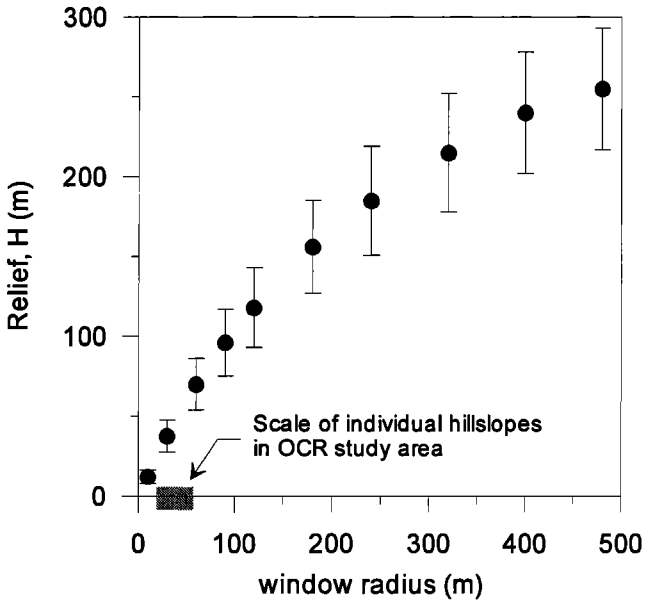


**Figure 6.** Plot of maximum relief as a function of window radius for the landscape depicted in Figure 2. Circles indicate the mean maximum relief calculated at evenly spaced points across the study area for a given window (or sampling) radius. The error bars indicate the standard deviation of maximum relief. The horizontal scale of hillslopes in the study site is ~ 20-50 m, such that the associated relief is ~ 30-60 m (15-20% of the total landscape relief).

### 6.2. Hillslope Adjustment to an Increase in the Rate of Baselevel Lowering

The following numerical experiment illustrates how hillslope morphology, sediment fluxes, and erosion rates respond to a step change in $C_o$. We used the OCR parameters ($K$=0.003 m$^2$ yr$^{-1}$, $S_c$=1.2, $L_h$=40 m, and $\rho_r/\rho_s$=2.0) to simulate how an equilibrium hillslope adjusts to a doubling in the channel incision rate (from $C_o$=5.0x10$^{-5}$ m yr$^{-1}$ to $C_o$=1.0x10$^{-4}$ m yr$^{-1}$). The corresponding values of $\Psi_L$ for the initial and final equilibrium hillslopes are 0.72 and 1.78, respectively, such that the relative importance of nonlinear transport increases and the final hillslope has a narrower zone of hilltop curvature and more planar sideslopes. Figure 7 depicts the temporal and spatial distribution of elevation, gradient, curvature, sediment flux, and erosion rate across the evolving hillslope. Initial and final equilibrium values of sediment flux at the hillslope base are denoted by $q_1$ and $q_2$, and the equilibrium values of erosion rate for the initial and final hillslope are denoted by $(C_o)_1$ and $(C_o)_2$, respectively. A step increase in $C_o$ causes slope angles at the base of the hillslope to steepen, increasing sediment flux into the channel network (Figures 7b and 7d). Increased erosion rates at the hillslope base cause the locally steepened section to propagate upslope, reaching the hillslope crest sometime after the initial change in the channel incision rate (Figure 7e). After the initial equilibrium state has been perturbed across the hillslope, further time is required for the hillslope to adjust its form to the newly imposed lowering rate, such that erosion rates become approximately constant (Figure 7e). In this example, the hillslope evolves from one with relatively little spatial variation in curvature to one with a highly convex crest and relatively planar sideslopes. At different points along the hillslope, curvature evolves along a complex path before reaching the final condition (Figure 7c). The final hillslope exhibits focused convexity at the hilltop. Figure 8 illustrates the temporal variation of sediment flux $q_L$ (measured at the base, $x=L_h$) and erosion rate at the hilltop $(\partial z/\partial t)_0$, both of which approach their new equilibrium value gradually. A similar hillslope response is observed for step changes in $K$ (when $C_o$ is held constant), although a different feedback mechanism controls the morphologic transformation. Specifically, a twofold increase in $K$ causes erosion rates across the hillslope to immediately double. Because channel

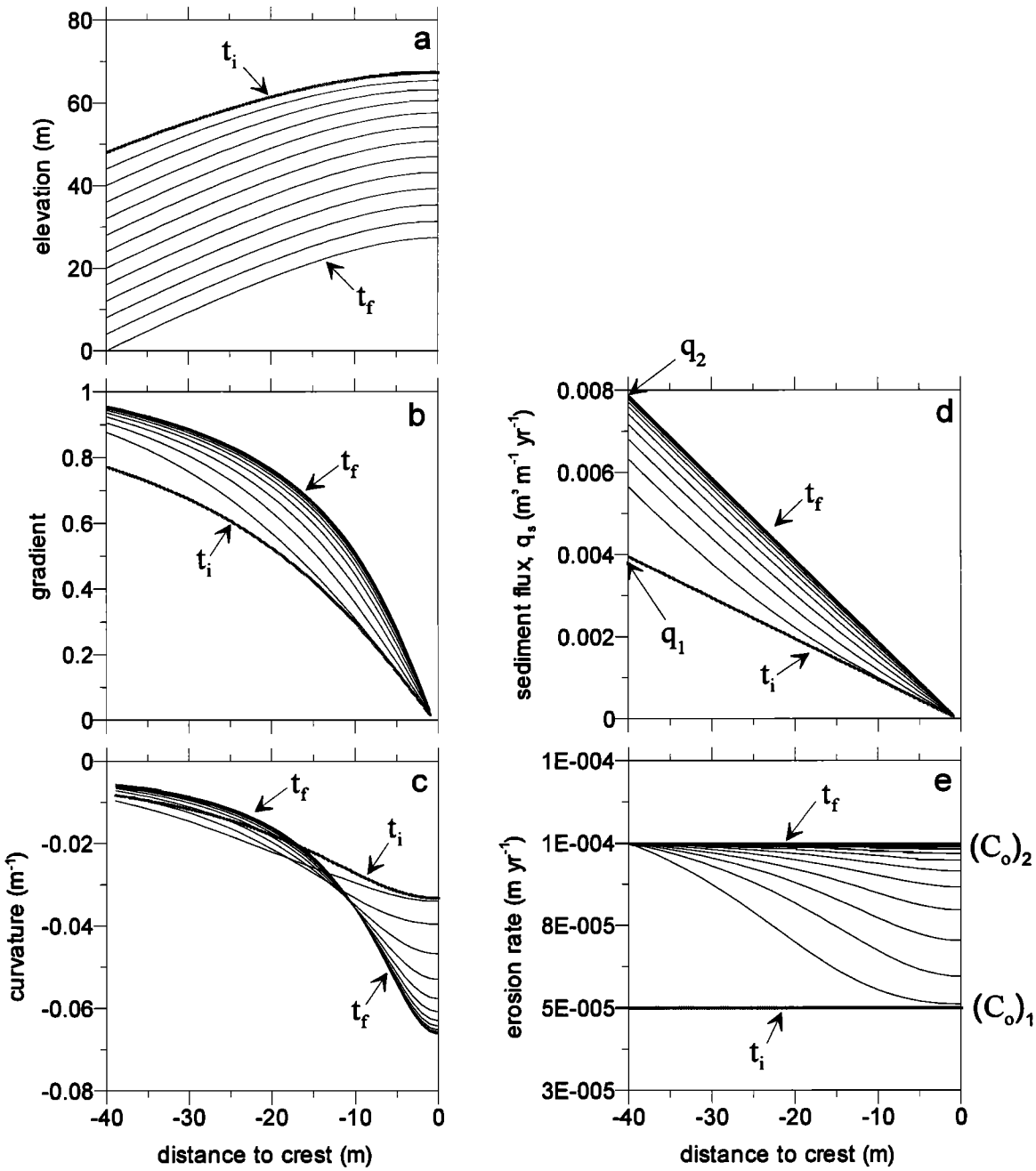


**Figure 7.** (a) Elevation, (b) gradient, (c) curvature, (d) sediment flux, and (e) erosion rate profiles of transient hillslope adjustment occurring after a twofold increase in baselevel lowering rate. The initial condition is an equilibrium profile with $C_o$=5.0x10$^{-5}$ m yr$^{-1}$, indicated by $t_i$ (thick shaded line), and the final condition (which is signifies the end of the simulation) is indicated by $t_f$. Model parameters are: $K$=0.003 m$^2$ yr$^{-1}$, $S_c$=1.2, $\rho_r/\rho_s$=1.0, and $L_h$ =40m. Profile lines are shown for 20 kyr increments. The clustering of profiles near $t_f$ illustrates the gradual approach to equilibrium. Read 1E-004 as 1x10$^{-4}$.

incision $C_o$ is held constant, the effect of differential erosion at the hillslope base propagates upslope (as in the previous case), such that the hillslope crest eventually adjusts its form to the constant incision rate and newly imposed value of $K$.

## 7. Equilibrium Definition and Evaluation

Although the concept of an equilibrium hillslope is appealing and intuitively accessible, defining and evaluating the attainment of approximate steady state topography is not a straightforward task [e.g., *Brunsden and Lin*, 1991; *Ahnert*, 1994; *Thorn and Welford*, 1994]. As elaborated by *Howard* [1988], equilibrium can be defined through a single-valued variable, such as gradient, curvature, or sediment flux. The choice of which variable to use depends on research goals and the spatial and temporal scales of available measurements. The numerical experiments of transient hillslope adjustment illustrated above (Figure 7) reveal two variables that may be diagnostic for defining equilibrium. Analogous to basin studies of sediment yield, sediment flux from hillslopes into

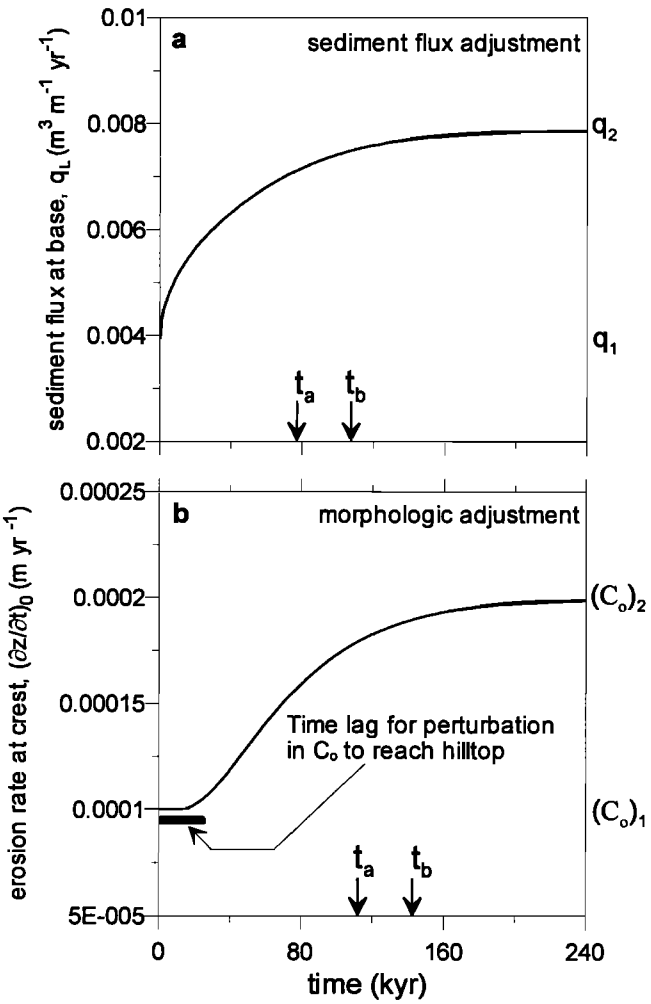


**Figure 8.** The variation of (a) sediment flux at the hillslope base $q_L$ and (b) erosion rate at the hillslope crest $(\partial z/\partial t)_0$ with time for the simulation shown in Figure 7. Arbitrary threshold-defined equilibrium adjustment times are shown by $t_a$ and $t_b$ for both time series of $q_L$ and $(\partial z/\partial t)_0$ (see text). The timescale $t_a$ indicates when $q_L$ or $(\partial z/\partial t)_0$ (evaluated independently) is within 10% of its final equilibrium value, $q_2$ or $(C_o)_2$ (equation (9)), and the timescale $t_b$ indicates the time when 90% of the change between the initial and final values of $q_L$ or $(\partial z/\partial t)_0$ (evaluated independently) is achieved (equation (10)). The thick shaded bar shown in (b) denotes the time lag for the perturbation in $C_o$ to reach the hillcrest, such that the final approach to morphologic equilibrium occurs after the approach to sediment flux equilibrium (see text).

the channel network ($q_L = q(L_h)$) can be used to evaluate equilibrium [*Reneau and Dietrich*, 1991; *Kooi and Beaumont*, 1996; *Fernandes and Dietrich*, 1997]. As shown in our example (Figures 7d and 7e), changes in incision rate are almost immediately transmitted to points along the base of the hillslope and the approximate attainment of the final equilibrium sediment flux does not necessarily reflect the status of morphologic adjustments upslope. In other words, the gradient (and thus sediment flux) near the base of a hillslope may adjust to its new equilibrium value before upslope sections of the hillslope have adjusted. Alternatively, a morphologic equilibrium definition may be used to define hillslope-wide adjustment, such that erosion rates across the entire hillslope are effectively constant and morphology is time-independent. To define this type of equilibrium, we evaluate $\partial z/\partial t$ at the hillslope crest ($x$=0), $(\partial z/\partial t)_0$, because it is the last landscape element to adjust to changes imposed at the hillslope-channel margin. Erosion rate at the crest is proportional to hillslope curvature, such that the time series of hilltop curvature would exhibit similar variation as $(\partial z/\partial t)_0$. For step changes in $C_o$ and $K$ the absolute time for morphologic equilibrium is longer than that for sediment flux equilibrium. The difference in time required to attain these two equilibrium states is approximately equal to the time required for the signal of the step change to propagate upslope and reach the hillslope crest (see Figure 8b).

### 7.1. Equilibrium Criteria

As our numerical example illustrates (Figure 8), sediment flux at the base $q_L$ and erosion rate at the crest $(\partial z/\partial t)_0$ approach their new equilibrium values, $q_2$ and $(C_o)_2$, asymptotically. As a result, we must devise a method for determining when the value of $q_L$ or $(\partial z/\partial t)_0$ is close enough to its new equilibrium value such that the variable may be considered effectively constant. *Howard* [1988] describes criteria for quantifying the time at which equilibrium is approximately attained for step changes in boundary conditions or model parameters (in our case $C_o$ and $K$). *Fernandes and Dietrich* [1997] used a simple threshold criterion to quantify the equilibrium adjustment time of hillslopes, $t_a$, that erode according to the linear transport model (equation (1)), such that equilibrium is achieved when $q_L$ or $(\partial z/\partial t)_0$ is within an arbitrary fraction of its final value, according to

$$t = t_a, \qquad |F(t) - F_2| \le PF_2 \tag{9}$$

where $F_2$ is the final equilibrium value of sediment flux or erosion rate, $q_2$ or $(C_o)_2$, respectively, $F(t)$ is the time-dependent value of $q_L$ or $(\partial z/\partial t)_0$, and $P$ is the threshold fraction used to define equilibrium (*Fernandes and Dietrich* [1997] used $P$=0.1). This approach may be problematic because initial perturbations that do not exceed the threshold fraction $P$ yield adjustment times of zero. Alternatively, equilibrium can be defined as the time when a certain fraction of the change between the initial and final states is achieved, $t_b$, according to

$$t = t_b, \qquad |F(t) - F_2| \le P|F_2 - F_1| \tag{10}$$

where $F_1$ is the initial equilibrium value of sediment flux or erosion rate, $q_1$ or $(C_o)_1$, respectively. We calculated equilibrium adjustment time (or relaxation time) according to these two definitions ((9) and (10)) for the hillslope evolution experiment depicted in Figure 7. For sediment flux equilibrium (defined by $q_L$), $t_a$=78 kyr and $t_b$=110 kyr, whereas for morphologic equilibrium (defined by $(\partial z/\partial t)_0$) $t_a$=113 kyr and $t_b$=143 kyr (using $P$=0.1) (Figure 8). As mentioned previously, these results demonstrate that for a given equilibrium criterion ($t_a$ or $t_b$) the absolute time for morphologic equilibrium exceeds the time for flux equilibrium, the difference being approximately equal to the time required for the signal of increased incision at the hillslope base to reach the crest (see Figure 8b). For this example the difference between morphologic and flux equilibrium is ~ 34 kyr.

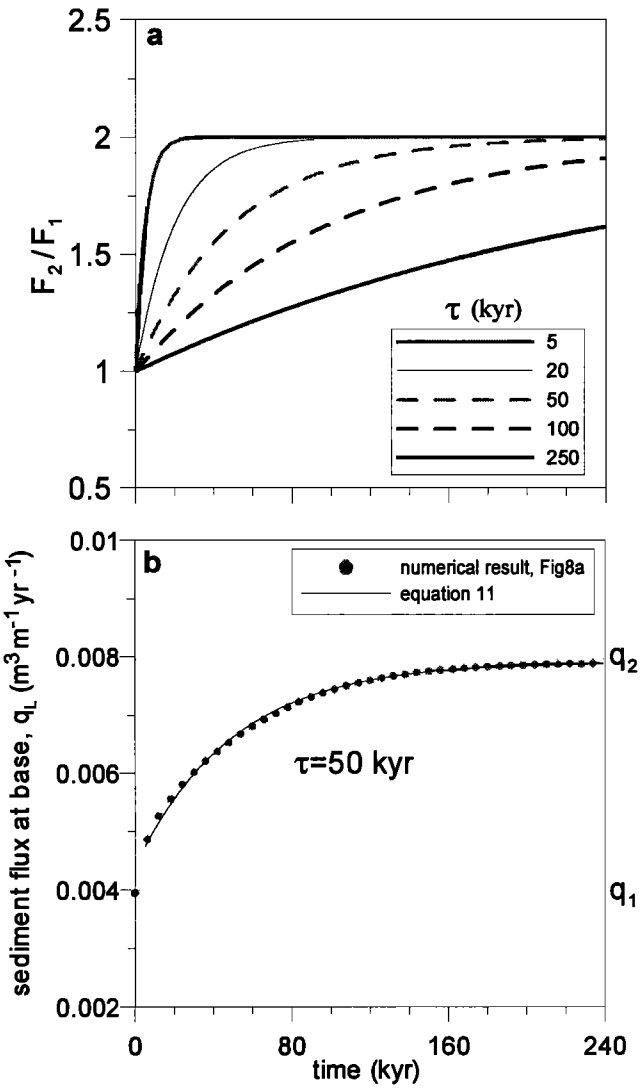


**Figure 9.** (a) Plot of (11) for various values of $t$ when $F_2/F_1$=2. (b) The transient response of sediment flux for a twofold increase in baselevel lowering, modeled with an exponential decay function (equation (11)). Small values of τ indicate a rapid approach, whereas large values correspond to longer, more gradual adjustments. Sediment flux for the simulation shown in Figures 7 and 8 (shaded dots) is well approximated by an exponential decay function with τ=50 kyr.

### 7.2. Exponential Approach to Equilibrium

The above described equilibrium criteria ((9) and (10)) are somewhat arbitrary and do not describe the characteristic behavior by which hillslopes gradually approach steady state (Figure 8). Following a step change in $C_o$ or $K$, time-dependent values of $q_L$ and $(\partial z/\partial t)_0$ can be well approximated with an exponential decay function [e.g., *Howard*, 1988], according to

$$F(t) = F_2 + (F_1 - F_2)e^{-t/\tau} \tag{11}$$

where the imposed step change occurs at $t$=0, $F$ is the variable used to define equilibrium (in our case $F$ will equal either $q_L$ or $(\partial z/\partial t)_0$), and τ is the exponential timescale that quantifies how rapidly $F$ approaches its final equilibrium value $F_2$. This approach enables us to describe transient behavior using an exponential timescale instead of an arbitrarily defined time threshold. Using (11), we calculated how different values of τ affect how $F$ approaches its final equilibrium value, $F_2/F_1$=2. Larger values of τ are associated with a slower approach to equilibrium and vice versa (Figure 9a). For the simulation depicted in Figures 7 and 8 we fit time-dependent values of $q_L$ with (11) and estimated that τ =50 kyr (Figure 9b). Because it provides a fairly complete and compact description of transient model behavior, we use τ to characterize the timescale for equilibrium adjustment. In the following analyses, we fit τ to time-dependent values of $q_L$ and $(\partial z/\partial t)_0$ as they approach their new equilibrium values. Furthermore, τ can be used to calculate time to equilibrium as defined by the previously discussed threshold criteria, $t_a$ and $t_b$ ((9) and (10)). By substituting (11) into (9) and (10), respectively, and solving for time $t$ we obtain [*Howard*, 1988]

$$t_a = -\tau \ln\left(\frac{P}{|F_1/F_2 - 1|}\right) \tag{12}$$

$$t_b = -\tau \ln(P) \tag{13}$$

If the response function is exponential, the time required to achieve an arbitrary fraction of the change between two equilibrium states is independent of the magnitude of the imposed change (equation (13)).

### 7.3. Analysis of Exponential Timescale: Linear Transport

To guide our investigation of how nonlinear transport influences the timescale for equilibrium adjustment, we used analytical equations that describe the transient behavior of linear diffusive boundary value problems and then used the ratio $\Psi_L$ to extend the analysis to nonlinear transport. Analytical solutions derived for transient, linear diffusive boundary value problems indicate that the exponential decay timescale in (11) τ should be proportional to $L_h^2/K$ [*Crank*, 1975]. Using the linear transport law (equation (1)) we modeled the exponential adjustment timescale τ associated with step changes in $C_o$ (baselevel lowering rate) and $K$ (transport rate constant) for hillslopes of various length $L_h$ and found that $\tau_{lin}$ (τ for linear transport) is well approximated by

$$\tau_{lin} = A\frac{L_h^2}{K} \tag{14}$$

where $A$ is a constant that we estimate to be 0.405 ±0.002 and $K$ is the transport rate constant used in the numerical model (Figure 10). Equation (14) provides us with a simple and compact description of how equilibrium adjustment time varies on hillslopes modeled by linear transport. The values of $\tau_{lin}$ shown in Figure 10 were estimated from both $q_L$ and $(\partial z/\partial t)_0$, indicating that for a given $L_h$ and $K$ the exponential timescale describing the final approach to equilibrium $\tau_{lin}$ is effectively equivalent for morphologic and flux equilibrium. To compare this result with those reported by *Fernandes and Dietrich* [1997], we used (12) and (14) to calculate the time required to evolve $q_L$ to within 10% of $q_2$ (equation (9)) for various step changes in $C_o$ and obtained results relating adjustment time $t_a$ to $L_h$, $K$, and the initial and final baselevel lowering rates (Table 1). Our results are nearly identical to those reported by *Fernandes and Dietrich* [1997] in a dimensionless graph.

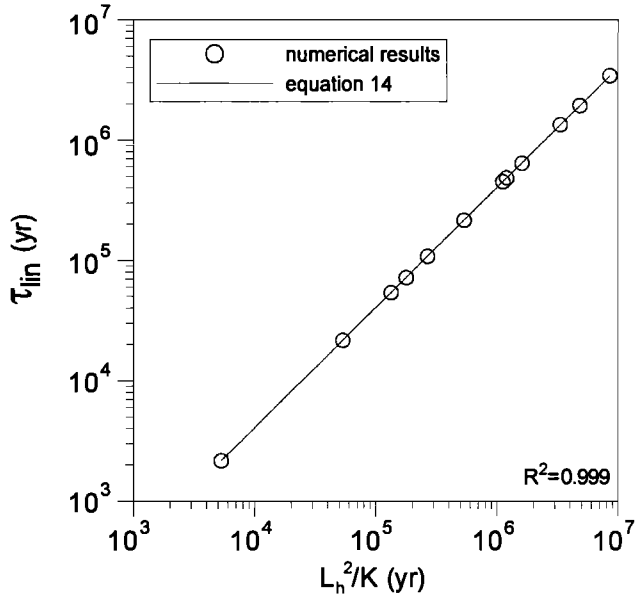


**Figure 10.** Variation of the exponential decay timescale with $L_h^2/K$ for hillslopes modeled with linear transport (equation (1)). Numerical results (open circles) are well approximated with linear relationship with slope A equal to 0.405 ±0.002.

### 7.4. Analysis of Exponential Timescale: Nonlinear Transport

To quantify how nonlinear transport affects $\tau$, we modeled the transient behavior of small perturbations in $C_o$ and/or $K$ for hillslopes with a range of $\Psi_L$ (which quantifies the relative importance of nonlinear transport, (8)). All else being equal, the timescale for adjustment to perturbations in $C_o$ and $K$ are essentially the same. In contrast to the twofold increase in $C_o$ illustrated in Figures 7 and 8 we used small perturbations for these simulations (imposed values of $C_o$ and/or $K$ differ from the initial values by < 1%). These small perturbations allow us to quantify how transient hillslope response varies with $\Psi_L$ because values of $\Psi_L$ for the initial and final equilibrium hillslopes are effectively equivalent. Using our numerical model, we simulated hillslope evolution with (2), using various hillslope lengths $L_h$, transport rate constants $K$, and incision rates $C_o$ and observed a nonlinear decrease in the exponential timescale $\tau_{non}$ with increasing $\Psi_L$ (Figure 11). We normalized our numerically derived estimates of $\tau_{non}$ with $\tau_{lin}$ calculated for a hillslope with the same values of $L_h$ and $K$ (equation (14)). As expected, for very small values of $\Psi_L$, $\tau_{non}/\tau_{lin} \cong 1$ because the relative importance of nonlinear transport is extremely small. With increasing $\Psi_L$, $\tau_{non}/\tau_{lin}$ decreases rapidly. This result indicates that nonlinear hillslope transport significantly decreases the time required for hillslopes to adjust to changing boundary conditions. The variation of $\tau_{non}$ with $\Psi_L$ is well described by the following nonlinear functions:

$$\frac{\tau_{non}}{\tau_{lin}} = \frac{1}{(1+\Psi_L)^B} \tag{15}$$

$$\tau_{non} = \frac{L_h^2}{K}\frac{A}{(1+\Psi_L)^B} \tag{16}$$

where $B$ is a constant that we estimate to be ~ 1.74 ±0.02 (Figure 11). Equation (16) allows us to estimate the timescale of equilibrium adjustment for hillslopes that erode by nonlinear slope-dependent transport. According to (15) and (16), for $\Psi_L >> 1$, equilibrium adjustments occur rapidly, although this analysis only applies where erosion rates do not outpace soil production. Thus the range of values of $\Psi_L$ relevant to real hillslopes is controlled by the ratio of the regolith production rate to the landscape lowering rate.

## 8. Discussion

Our analysis of nonlinear transport and steady state slope morphology indicates that equilibrium hillslope relief and slope angle are poor indicators of tectonic forcing (Figure 5). On steep slopes, decreasing frictional resistance (and possibly shallow landsliding) causes transport rates to increase rapidly for small increases in slope angle, such that large increases in erosion rate may be accommodated by small slope increases. Consistent with our analysis, recent field studies demonstrate that in steep, mountainous landscapes, erosion rates vary several-fold with little change in hillslope angles [*Burbank et al.*, 1996; *Whipple et al* , 1999]. For a given hillslope length, nonlinear models predict that above a particular erosion rate, hillslope relief does not vary widely with erosion rate. For our calculations using parameters characteristic of the Oregon Coast Range and other soil-mantled landscapes the difference between hillslope relief calculated by the linear and nonlinear models increases dramatically for erosion rates >5x10$^{-4}$ m yr$^{-1}$. Individual hillslopes constitute a relatively small amount of the total landscape relief in the Oregon Coast Range study site (15-20%), such that valley incision by debris flows [*Stock and Dietrich*, 1999] and network evolution are likely to regulate long-term relief development.

Although other nonlinear transport models have been proposed, we use (2) in this study because it has been tested and field calibrated over the relevant spatial scale. Once calibrated, other nonlinear models that include a term to describe the critical gradient at which sediment flux approaches infinity or a maximum value [*Kirkby*, 1984;

**Table 1.** Comparison of Hillslope Adjustment Times Modeled with the Linear Transport Model: This Study and *Fernandes and Dietrich* [1997]

| Final/Initial | $t_a$, kyr | |
|---|---|---|
| Lowering Rate $(C_o)_2/(C_o)_1$ | This Study | Fernandes and Dietrich |
| 10 | 475 | 460 |
| 2 | 347 | 330 |
| 0.1 | 973 | 1,020 |
| 0.01 | 1,490 | 1,540 |

Here $t_a$ is defined according to (9) where $P$=0.1. $K$=0.003 m$^2$ yr$^{-1}$ for all calculations.
For this study, $t_a$ is calculated using (12) and (14).
For Fernandes and Dietrich, $t_a$ is estimated using Figure 9 of *Fernandes and Dietrich* [1997].

*Anderson*, 1994; *Howard*, 1994] produce results nearly identical to those shown here. *Andrews and Bucknam* [1987] proposed another nonlinear transport model without a critical gradient term. Such models predict that high-relief, steady state hillsides gradually steepen without limit in the downslope direction, although the magnitude of steepening may be imperceptible on sufficiently long natural slopes.

The equilibrium concept must be applied to hillslopes over the appropriate temporal and spatial scales. Recognizing that considerable fluctuations may prevail over shorter length scales, numerous studies have applied the equilibrium concept to characterize tectonic forcing across entire mountain ranges [e.g., *Koons*, 1989; *Brunsden and Lin*, 1991; *Anderson*, 1994; *Whipple et al.*, 1999]. Hillslopes supply sediment to channels, thereby controlling the sediment load that affects fluvial incision downstream [*Sklar and Dietrich*, 1999]. Our analysis suggests that hillslope adjustment is highly sensitive to the length scale (or spatial extent) of individual hillslopes and the relative importance of nonlinear transport processes. In highly dissected landscapes with steep, threshold-controlled slopes (e.g., the Oregon Coast Range), hillslopes account for a small portion of the total relief and adjust rapidly to changes in the rate of channel incision. In contrast, broad, gentle hillslopes in poorly dissected terrain account for a larger proportion of the landscape relief and have long adjustment times.

Our results demonstrate that relative to the widely used linear model, nonlinear hillslope transport reduces the timescale for equilibrium adjustment to changes in incision rate $C_o$ and to changes in the climate-dependent hillslope transport rate constant $K$. As $\Psi_L$ becomes large (i.e., the relative importance of nonlinear transport increases), the timescale decreases rapidly, and the relationship between $\Psi_L$ and $\tau_{non}/\tau_{lin}$ is well approximated by a power law function with an exponent equal to approximately -1.74 (see (15)). However, our analysis applies only to soil-mantled hillslopes, such that landscape lowering rates do not exceed rates of soil production. Recent analyses of soil production using cosmogenic radionuclides indicate that hillslopes may be soil-mantled for landscape lowering rates $< 2.0\text{x}10^{-3}$ m yr$^{-1}$ [*Heimsath*, 1999]. This upper bound presumably varies with lithology and surface processes. In some high-relief landscapes, erosion rates greatly exceed $2.0\text{x}10^{-3}$ m yr$^{-1}$, and the dominant denudational processes are thought to be bedrock landsliding and/or glacial erosion [*Burbank et al.*, 1996; *Brozovic et al.*, 1997]. Our analysis does not account for the mechanics of bedrock toppling, structurally controlled rockfalls, deep-seated landsliding, or glacial abrasion, all processes that may be characteristic of high mountain landscapes.

Our analysis uses an exponential decay approach to quantify hillslope adjustment to changes in tectonic forcing, similar to previous studies [e.g., *Kooi and Beaumont*, 1996]. For our analysis of nonlinear transport and transient adjustment, we simplified the influence of nonlinear transport by modeling small perturbations in lowering rates, such that the initial and final hillslopes had very similar values of $\Psi_L$. For hillslopes that undergo a large step change in incision rate (such that the initial and final equilibrium hillslopes have significantly different values of $\Psi_L$) the adjustment timescale $\tau$ will vary nonlinearly as the hillslope evolves. The initial period of response will reflect the exponential timescale associated with $\Psi_L$ for the initial hillslope, whereas the final approach to equilibrium is well approximated by $\Psi_L$ for the final equilibrium hillslope. Because the final equilibrium approach ultimately determines the time for adjustment, the value of $\Psi_L$ for the final equilibrium hillslope is most applicable for analyzing hillslope evolution. For example, our initial simulation (Figures 7 and 8) describes how a hillslope evolves from an initial condition with $\Psi_L$=0.72 to a final condition with $\Psi_L$=1.78, such that $\tau_{non}$ changes from 84 to 36 kyr through the course of the simulation (as calculated with (16)). As shown in Figure 9b, we can fit the entire time series of $q_L$ with (11) using $\tau$=50 kyr, although early portions of the curve are better approximated using $\tau$=84 kyr and later portions are better approximated using $\tau$=36 kyr (see Figure 11). When compared to the adjustment timescale predicted by linear transport ($\tau_{lin}$=216 kyr) and additional uncertainties inherent to models of landscape evolution, the temporal variation in $\tau_{non}$ as a hillslope evolves may be relatively small.

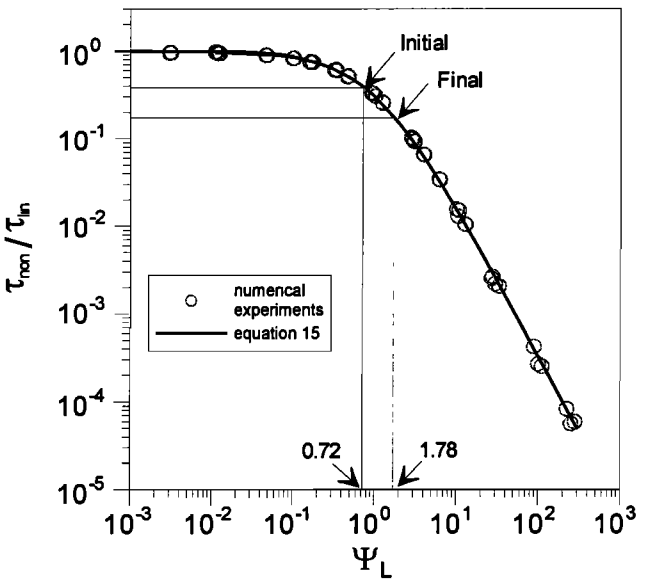


**Figure 11.** Variation of $\tau_{non}/\tau_{lin}$ with $\Psi_L$ for hillslopes modeled with various values of $K$ and $C_o$. For small $\Psi_L$ the nonlinear and linear adjustment timescales are effectively equivalent, whereas for increasing $\Psi_L$ the adjustment timescale decreases rapidly. The relationship is well approximated by (15), with the exponent approximately equal to 1.74±0.02. The thin solid lines show the initial and final values of $\Psi_L$ (initial value of 0.72; final value of 1.78) and

Systematic analysis of adjustment timescales associated with geomorphic processes may improve our ability to evaluate whether uplift and erosion are approximately balanced in a particular landscape. In the Oregon Coast Range our results indicate that the characteristic hillslope adjustment timescale $\tau$ is approximately 50 kyr, which is more than a factor of 4 shorter than the adjustment timescale predicted by linear transport (216 kyr). This suggests that individual hillslopes adjust more rapidly to changing boundary conditions than previously proposed, such that the morphologic adjustment of steep, soil-mantled landscapes may ultimately be limited by the ability of the channel network to transmit the signal of baselevel lowering. *Whipple and Tucker* [1999] used the stream power equation to quantify the adjustment of channel networks to changes in the rate of baselevel lowering and demonstrated that basin response varies significantly with the model parameters

describing channel incision. Future studies will combine fluvial erosion models and hillslope transport models to analyze transient coupling between hillslopes and channels. Recent studies have attempted to quantify rates of uplift and denudation in mountainous landscapes and evaluate the likelihood of steady state topography [e.g., *Hovius et al.*, 1997; *Meigs et al.*, 1999; *Riebe et al.*, 2000]. As stated in these contributions, erosional adjustment timescales control landscape response to tectonic forcing and thus the time required for denudation to balance uplift.

Although the exponential timescale that describes the final approach to equilibrium is the same for the sediment flux and morphologic equilibrium definitions, adjustment of the hilltop does not begin until the perturbation induced by a boundary condition change propagates upslope. As a result, the morphologic adjustment lags behind that of sediment flux. As illustrated in Figure 8b, the magnitude of this lag is small compared to the equilibrium adjustment timescale. By analogy, estimates of basin-wide sediment yield in mountainous terrain may not be indicative of time-independent landscape morphology [e.g., *Meigs et al.*, 1999; *Reneau and Dietrich*, 1991]. Instead, the upland landscape morphology may reflect previous tectonic and/or climatic conditions. Furthermore, estimates of sediment yield may reflect changes in sediment storage for specific elements of a drainage basin (e.g., floodplains) and not morphologic adjustment of hillslopes.

Complicated patterns of tectonic and climatic forcing undoubtedly influence the erosional response of landscapes. As described by *Howard* [1988], oscillatory fluctuations in climate or tectonics may introduce complex relationships between landscape morphology and tectonic or climatic forcing. The manifestation of such fluctuations likely depends on the amplitude and wavelength of boundary condition variations relative to the landscape adjustment timescale. Our analysis may be easily adapted to incorporate such variability, but owing to the lack of geologic evidence indicating such variability we do not include those effects in this study.

## 9. Conclusions

Hillslope morphology reflects the interaction between surface processes and tectonic and climatic forcing. Soil-mantled hillslopes respond to changes in baselevel lowering and/or climatic conditions by adjusting their morphology such that erosion rates approach a constant value across the hillslope. From our simulations of hillslope evolution by nonlinear slope-dependent transport we conclude the following:

1. Contrary to predictions of the frequently used linear transport model, our proposed nonlinear model indicates that hillslope relief and gradient are not sensitive indicators of tectonic forcing. For model parameters and erosion rates characteristic of the Oregon Coast Range and other soil-mantled landscapes, relief and average slope angle will increase only 10% for a twofold increase in erosion rate. However, our nonlinear model indicates that hilltop curvature varies proportionally with erosion rate and may be diagnostic for inferring tectonic forcing from hillslope morphology.

2. We quantify the relative importance of nonlinear transport with a dimensionless parameter, $\Psi_L$ (defined as the ratio of nonlinear to linear components of sediment flux at the hillslope base), where low values of $\Psi_L$ reflect steady state hillslopes with relatively constant curvature between the crest and channel and high values characterize hillslopes with narrow, highly convex hilltops and relatively planar sideslopes.

3. Hillslope adjustments to step changes in baselevel lowering or the climate-related hillslope transport rate constant are well approximated by an exponential decay function. For the linear model the exponential time constant varies with the square of hillslope length and the inverse of the transport rate constant. Nonlinear transport on hillslopes decreases the equilibrium adjustment timescale. On hillslopes where the magnitude of nonlinear transport is relatively small, the adjustment timescale is similar to that for linear transport, whereas with increasing importance of nonlinear transport the adjustment timescale decreases rapidly. In our Oregon Coast Range study site the relief associated with individual hillslopes is ~ 15-20% of the total landscape relief and the nonlinear transport model predicts that hillslopes adjust rapidly to changes in baselevel lowering (4 times faster than previously predicted with the linear transport model). Considered together, these results suggest that in steep, soil-mantled landscapes the signal of tectonic forcing may be quickly assimilated by hillslopes, such that channel incision and the coupling of hillslopes and channels may ultimately control the adjustment of entire drainage basins.

**Acknowledgments.** We thank C. Riebe for insightful discussions and R. Arrowsmith and A. Crave for thorough and constructive review comments. This work was supported by NSF grants EAR-9357931 and EAR-9614442 to J.W.K.

## References

Ahnert, F., Functional relationships between denudation, relief and uplift in large, mid-latitude drainage basins, *Am. J. Sci.*, *268*, 243-263, 1970.

Ahnert, F., Brief description of a comprehensive three-dimensional process-response model of landform development, *Z. Geomorphol. Suppl.*, *25*, 29-49, 1976.

Ahnert, F., Approaches to dynamic equilibrium in theoretical simulations of slope development, *Earth Surf. Processes Landforms*, *12*, 3-15, 1987.

Ahnert, F., Equilibrium, scale and inheritance in geomorphology, *Geomorphology*, *11*, 125-140, 1994.

Anderson, R.S., Evolution of the Santa Cruz Mountains, California, through tectonic growth and geomorphic decay, *J. Geophys. Res.*, *99*, 20,161-20,174, 1994.

Andrews, D.J., and R.C. Bucknam, Fitting degradation of shoreline scarps by a nonlinear diffusion model, *J. Geophys. Res.*, *92*, 12,857-12,867, 1987.

Baldwin, E.M., Geologic map of the lower Siuslaw River area, Oregon, *U.S. Geol. Surv. Oil Gas Invest. Map, OM-186*, 1956.

Benda, L., and T. Dunne, Stochastic forcing of sediment supply to channel networks from landsliding and debris flow, *Water Resour. Res.*, *33*, 2849-2863, 1997.

Brozovic, N., D. Burbank, and A. Meigs, Climatic limits on landscape development in the northwestern Himalaya, *Science*, *276*, 571-574, 1997.

Brunsden, D., and J.C. Lin, The concept of topographic equilibrium in neotectonic terrains, in *Neotectonics and Resources*, edited by J.W. Cosgrove, pp. 120-143, Belhaven, London, 1991.

Burbank, D.W., J. Leland, E. Fielding, R.S. Anderson, N. Brozovic, M.R. Reid, and C. Duncan, Bedrock incision, rock uplift and threshold hillslopes in the Northwestern Himalayas, *Nature*, *379*, 505-510, 1996.

Carson, M.A., and D.J. Petley, The existence of threshold hillslopes in the denudation of the landscape, *Trans. Inst. Br. Geogr.*, *49*, 71-95, 1970.

Crank, J., *The Mathematics of Diffusion*, Clarendon, Oxford, England, 1975.
Culling, W.E.H., Analytical theory of erosion, *J. Geol.*, *68*, 336-344, 1960.
Davis, W.M., The convex profile of badland divides, *Science*, *20*, 245, 1892.
Dietrich, W.E., and T. Dunne, Sediment budget for a small catchment in mountainous terrain, *Z. Geomorphol. Suppl.*, *29*, 191-206, 1978.
Dietrich, W.E., and D.R. Montgomery, Hillslopes, channels, and landscape scale, in *Scale Dependence and Scale Invariance in Hydrology*, edited by G. Sposito, pp. 30-60, Cambridge Univ. Press, New York, 1998.
Dietrich, W.E., C.J. Wilson, D.R. Montgomery, J. McKean, and R. Bauer, Erosion thresholds and land surface morphology, *Geology*, *20*, 675-679, 1992.
Dietrich, W.E., R. Reiss, M.-L. Hsu, and D.R. Montgomery, A process-based model for colluvial soil depth and shallow landsliding using digital elevation data, *Hydrol. Processes*, *9*, 383-400, 1995.
Fernandes, N.F., and W.E. Dietrich, Hillslope evolution by diffusive processes: The timescale for equilibrium adjustments, *Water Resour. Res.*, *33*, 1307-1318, 1997.
Fourier, J.B.J., *Théorie Analytique de la Chaleur*, F. Didot, Paris, 1822.
Gilbert, G.K., Report on the geology of the Henry Mountains (Utah), Survey of the Rocky Mountains Region, U.S. Geol. Surv., 1877.
Gilbert, G.K., The convexity of hilltops, *J. Geol.*, *17*, 344-350, 1909.
Granger, D.E., J.W. Kirchner, and R. Finkel, Spatially averaged long-term erosion rates measured from in-situ produced cosmogenic nuclides in alluvial sediment, *J. Geol.*, *104*, 249-257, 1996.
Hack, J.T., Interpretation of erosional topography in humid temperate regions, *Am. J. Sci.*, *258*, 80-97, 1960.
Heimsath, A.M., The soil production function, Ph.D. thesis, 324 pp., Univ. of California, Berkeley, Berkeley, 1999.
Heimsath, A.M., W.E. Dietrich, K. Nishiizumi, and R.C. Finkel, The soil production function and landscape equilibrium, *Nature*, *388*, 358-361, 1997.
Heller, P.L., Z.E. Peterman, J.R. O'Neil, and M. Shafiqullah, Isotopic provenance of sandstones from the Eocene Tyee Formation, Oregon Coast Range, *Geol. Soc. Am. Bull.*, *96*, 770-780, 1985.
Hovius, N., C.P. Stark, and P.A. Allen, Sediment flux from a mountain belt derived by landslide mapping, *Geology*, *25*, 231-234, 1997.
Howard, A.D., Equilibrium models in geomorphology, in *Modelling Geomorphological Systems*, edited by M.G. Anderson, pp. 49-72, John Wiley, New York, 1988.
Howard, A.D., A detachment-limited model of drainage basin evolution, *Water Resour. Res.*, *30*, 2261-2285, 1994.
Howard, A.D., Badland morphology and evolution: Interpretation using a simulation model, *Earth Surf. Processes Landforms*, *22*, 211-227, 1997.
Howard, A.D., and G. Kerby, Channel changes in badlands, *Geol. Soc. Am. Bull.*, *94*, 739-752, 1983.
Hurtrez, J.-E., F. Lucazeau, J. Lave, and J.-P. Avouac, Investigation of the relationships between basin morphology, tectonic uplift, and denudation from the study of an active fold belt in the Siwalik Hills, central Nepal, *J. Geophys. Res.*, *104*, 12,779-12,796, 1999.
Kirkby, M.J., Hillslope process-response models based on the continuity equation, *Inst. Br. Geogr. Spec. Publ.*, *3*, 15-30, 1971.
Kirkby, M.J., Modelling cliff development in South Wales; Savigear re-reviewed, *Z. Geomorphol.*, *28*, 405-426, 1984.
Kooi, H., and C. Beaumont, Large-scale geomorphology: Classical concepts reconciled and integrated with contemporary ideas via a surface processes model, *J. Geophys. Res.*, *101*, 3361-3386, 1996.
Koons, P.O., The topographic evolution of collisional mountain belts: A numerical look at the Southern Alps, New Zealand, *Am. J. Sci.*, *289*, 1041-1069, 1989.
McKean, J.A., W.E. Dietrich, R.C. Finkel, J.R. Southon, and M.W. Caffee, Quantification of soil production and downslope creep rates from cosmogenic $^{10}$Be accumulations on a hillslope profile, *Geology*, *21*, 343-346, 1993.
Meigs, A., N. Brozovic, and M.L. Johnson, Steady, balanced rates of uplift and erosion of the Santa Monica Mountains, California, *Basin Res.*, *11*, 59-73, 1999.
Milliman, J.D., and J.P.M. Syvitski, Geomorphic/tectonic control of sediment discharge to the ocean: The importance of small mountainous rivers, *J. Geol.*, *100*, 525-544, 1992.
Montgomery, D.R., and W.E. Dietrich, Source areas, drainage density, and channel initiation, *Water Resour. Res.*, *25*, 1907-1918, 1989.
Montgomery, D.R., and W.E. Dietrich, Channel initiation and the problem of landscape scale, *Science*, *255*, 826-830, 1992.
Orr, E.L., W.N. Orr, and E.M. Baldwin, *Geology of Oregon*, Kendall/Hunt, Dubuque, Iowa, 1992.
Press, W.H., S.A. Teukolsky, W.T. Vetterling, and B.P. Flannery, *Numerical Recipes in C: The Art of Scientific Computing*, Cambridge Univ. Press, New York, 1992.
Reneau, S.L., and W.E. Dietrich, Erosion rates in the Southern Oregon Coast Range: Evidence for an equilibrium between hillslope erosion and sediment yield, *Earth Surf. Processes Landforms*, *16*, 307-322, 1991.
Riebe, C.S., J.W. Kirchner, D.E. Granger, and R.C. Finkel, Erosional equilibrium and disequilibrium in the Sierra Nevada mountains, inferred from cosmogenic $^{26}$Al and $^{10}$Be alluvial sediment, *Geology*, *28*, 803-806, 2000.
Rinaldo, A., W.E. Dietrich, R. Rigon, G.K. Vogel, and I. Rodriguez-Iturbe, Geomorphological signatures of varying climate, *Nature*, *374*, 632-635, 1995.
Roering, J.J., J.W. Kirchner, and W.E. Dietrich, Evidence for nonlinear, diffusive sediment transport on hillslopes and implications for landscape morphology, *Water Resour. Res.*, *35*, 853-870, 1999.
Roering, J.J., J.W. Kirchner, L.S. Sklar, and W.E. Dietrich, Hillslope evolution by nonlinear creep and landsliding: An experimental study, *Geology, 29*, 143-146, 2001.
Sklar, L., and W.E. Dietrich, River longitudinal profiles and bedrock incision models: Stream power and the influence of sediment supply, in *Rivers Over Rock: Fluvial Processes in Bedrock Channels*, Geophys. Monogr. Ser., vol. 107, edited by K.J. Tinkler, and E.E. Wohl, pp. 237-260, AGU, Washington, D.C., 1999.
Small, E.E., R.S. Anderson, and G.S. Hancock, Estimates of the rate of regolith production using $^{10}$Be and $^{26}$Al from an alpine hillslope, *Geomorphology*, *27*, 131-150, 1999.
Snavely, P.D., H.C. Wagner, and N.S. MacLeod, Rhythmic-bedded eugeosynclinal deposits of the Tyee Formation, Oregon Coast Range, *Kans. Geol. Surv. Bull.*, *169*, 461-480, 1964.
Stock, J.D., and W.E. Dietrich, Valley incision by debris flows: Field evidence and hypotheses linking flow frequency to morphology, *Eos Trans. AGU, 80(46)*, Fall Meet. Suppl., F473, 1999.
Strahler, A.N., Equilibrium theory of erosional slopes approached by frequency distribution analysis, *Am. J. Sci.*, *248*, 673-696, 1950.
Thorn, C.E., and M.R. Welford, The equilibrium concept in geomorphology, *Ann. Assoc. Am. Geogr.*, *84*, 666-696, 1994.
Tucker, G.E., and R.L. Bras, Hillslope processes, drainage density, and landscape morphology, *Water Resour. Res.*, *34*, 2751-2764, 1998.
Tucker, G.E., and R.L. Slingerland, Erosional dynamics, flexural isostasy, and long-lived escarpments: A numerical modeling study, *J. Geophys. Res.*, *99*, 12,229-12,243, 1994.
Whipple, K.X., and G.E. Tucker, Dynamics of the stream-power river incision model: Implications for height limits of mountain ranges, landscape response timescales, and research needs, *J. Geophys. Res.*, *104*, 17,661-17,674, 1999.
Whipple, K.X., E. Kirby, and S.H. Brocklehurst, Geomorphic limits to climate-induced increases in topographic relief, *Nature*, *401*, 39-43, 1999.
Willgoose, G., R.L. Bras, and I. Rodriguez-Iturbe, Results from a new model of river basin evolution, *Earth Surf. Processes Landforms*, *16*, 237-254, 1991.

W. Dietrich and J. Kirchner, Department of Earth and Planetary Science, University of California, Berkeley, Berkeley, CA 94720-4767. (bill@seismo.berkeley.edu; kirchner@seismo.berkeley.edu)

J. Roering, Department of Geological Sciences, University of Oregon, Eugene, OR 97403-1272. (jroering@stanfordalumni.org)

(Received June 5, 2000; revised January 22, 2001; accepted March 28, 2001.)